

# Fatigue analysis of catenary contact wires for high speed trains

J.P. Massat\*, T.M.L. Nguyen-Tajan\*, H. Maitournam<sup>†</sup> and E. Balmès<sup>‡</sup>

\*: Research Department, French Railways (SNCF), Paris, France

<sup>†</sup>: Laboratory for the Mechanics of Solids – Ecole Polytechnique

<sup>‡</sup>: SDTools/Arts et Métiers ParisTech

Corresponding author: Jean-Pierre Massat (jean-pierre.massat@sncf.fr), Direction de l'Innovation et de la Recherche, 45, rue de Londres, 75379, Paris Cedex 08, FRANCE

*The fatigue fracture is one of the most critical failures which may occur on the high speed network because it is undetectable and it has a huge impact on traffic disruption. The contact wire lifespan of a high speed line is estimated at more than 50 years and thus it is necessary to consider the risk of fatigue. The Railway Technical Research Institute in Japan studied this phenomenon for a long time and performed experimental tests. Using these results and by comparing with failures occurred in France, a preliminary analysis is carried out to identify parameters which significantly influence the fatigue phenomenon. This analysis consists in using the numerical software OSCAR<sup>®</sup> to evaluate the loads, perform a fatigue assessment of the contact wire. The procedure, using a one-dimensional and a three-dimensional model, is described in this article.*

**Keywords:** Overhead Contact Line (OCL), hard drawn copper contact wire, fatigue failure, Dang Van's criterion, Finite Element volume mesh.

## 1 Introduction

Nowadays, the main criterion used to determine the contact wire replacement of the Overhead Contact Line (OCL) is wear but, on high speed lines, the measured wear rate is very small. In this way, the contact wire lifespan of a high speed line is estimated at more than 50 years and thus it is necessary to consider the risk of having other types of system failure.

The fatigue fracture is one of the most critical failures which may occur on the high speed network because it is undetectable and it has a huge impact on traffic disruption, client discomfort (delays, speed slowdowns) and cost explosion. Unfortunately, conditions of use increase the risk of fatigue failure:

- with overloaded traffic, each year more than 220 000 pantographs run under the catenary between Paris and Lyon,
- the tensile load applied to the contact wire is very high particularly on high speed lines and may increase in the future,
- the damping ratio of the catenary is so low that a loading cycle is composed of several bending waves preceding and following the pantograph passage,
- there is a lot of defects in the contact wire surface due to pantograph friction, electrical arcs and corrosion which can cause crack initiation (see. Figure 1a, b & c).

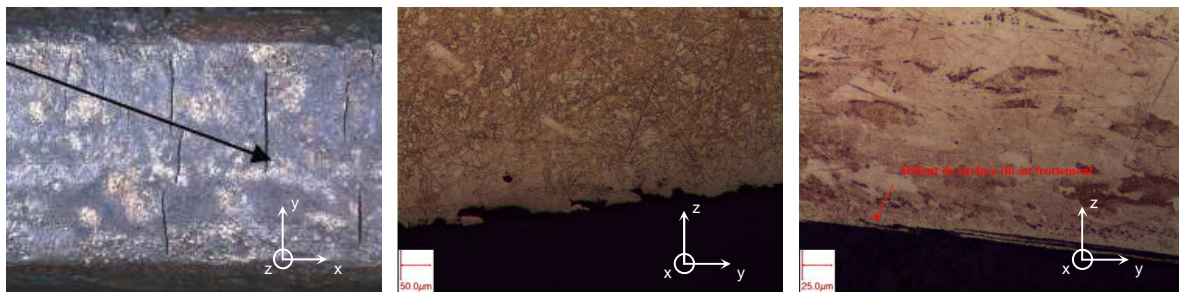


**Figure 1a. (left) Crack initiations and surface defects in the contact wire;**  
**Figure 1b. (centre) micrographic section of the contact wire: specks due to electrical arcs;**  
**Figure 1c. (right) micrographic section of the contact wire: surface defects due to friction.**

In France, some fatigue failures have already occurred on the overhead contact line between Paris and Lyon. This overhead line was replaced after only 29 years of use because fatigue failures took

place under the junction claws. This component, commonly used in maintenance on classical lines, appeared to be inadequate when used on high speed lines. Its heavy weight and its high stiffness produce important dynamic loads and arcing with the pantograph passage. A modification of the maintenance procedure limits the number of settled claws and their duration, but the fatigue could take place on other lines.

Indeed, the French network speed rising tendency requires an increase of the mechanical tension in the contact wire and this parameter heightens the fatigue failure phenomenon.

The RTRI<sup>1</sup>, one of the research departments of Japan railways, studied the fatigue failure of the contact wire for a long time, see [1], [2] and [3]. They developed a specific test bench and performed inline tests in order to measure and study the stress cycles in the contact wire. A comparison of the different approaches is led over the partnership between RTRI and SNCF.

In this paper, we show the numerical study developed by SNCF using experimental results of RTRI as reference. The numerical study was carried out using OSCAR<sup>®2</sup>, the pantograph-catenary dynamic interaction simulation software developed at SNCF and based on Finite Elements (FE) method [4]. This tool is used to compute dynamic loads in the catenary using 1D finite element and to deduce the zone of maximum uniaxial stresses along the catenary. A fully 3D contact wire model of this selected zone is then built to study the multiaxial stress history in the contact wire section [5].

## 2 Preliminary analysis

In this section, results of inline fatigue failure obtained on the French network and on the test bench of RTRI are compared. Using this preliminary analysis, it appears that the phenomena are complex and difficult to predict.

Indeed, contact wire failure which occurred inline (next to a claw) are different from those obtained using the test bench of RTRI. In both cases, the fatigue failure process follows three stages: crack initiation, crack propagation and failure. This last step occurs when the material that has not been affected by the crack cannot withstand the applied stress. One can determine material failed by fatigue by examining the appearance of the fracture. A fatigue fracture will have two distinct regions; one being smooth or burnished as a result of the rubbing of the bottom and top of the crack; the second is granular, due to the rapid failure of the material. These visual clues may be seen in Figure 3 and Figure 5a but these figures illustrate significant differences between test bench and inline failure.

### 2.1 Contact wire fatigue fracture on test bench

The RTRI research department built a specific test bench to study fatigue breakage phenomenon [2]. This test bench described in the Figure 2 was designed to reproduce realistic operation conditions by using a sample of real contact wire, by adding a tensile load on the contact wire to obtain the relevant mean stress and by applying a representative bending stress controlled by deformation.

Considering the test is performed on a sample of a real contact wire, without any machining and thus with a constant section, a three bending point bench was chosen to force the fatigue failure to take place under the oscillating roller as described in Figure 2. In this way, it is easier to stick sensors close to the crack initiation point.

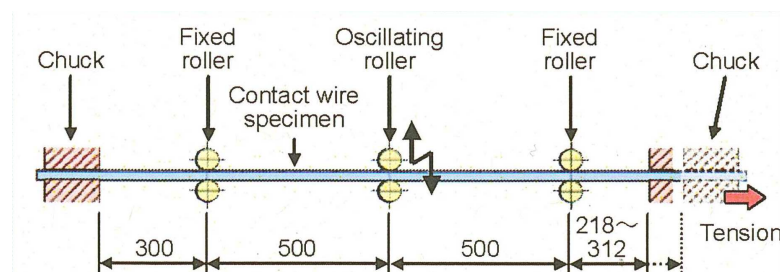
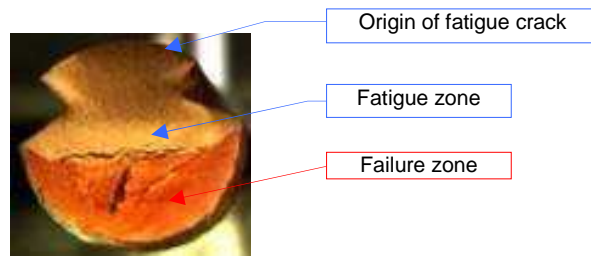


Figure 2. RTRI test bench for OCL contact wire study [2].

Some tests were made on this bench using samples of OCL contact wire provided by SNCF. This was a hard drawn copper contact wire used on high speed lines and its section was  $150\text{mm}^2$ . The tensile load applied was 19.6kN.

<sup>1</sup> Railway Technical Research Institute

<sup>2</sup> OSCAR : Outil de Simulation du CAptage pour la Reconnaissance des défauts



**Figure 3. Fatigue fracture obtained on the RTRI's bench.**

The fatigue crack appearance is shown in Figure 3. The three steps of the fatigue process can be identified: crack initiation, crack propagation and failure. The origin of the fatigue crack occurred on the top of the contact wire. Indeed, a dark area corresponding to crack initiation begins on the upper edge of the wire and the crack propagates to failure by necking of the wire. One can note that these tests are reproducible and evolution of the fatigue fracture appearance remains independent of the bending strain amplitude.

## 2.2 Inline fatigue failure analysis

The behaviour described above is different from that obtained inline though contact wire is similar. This may be explained because all inline fatigue failures on the French network occurred under a junction claw (see Figure 4).



**Figure 4. Photos of a junction claw.**

This component is used to connect two contact wires because of a breakage or to reinforce a weak point of the wire. Its mass is greater than the apparent mass of the catenary. When the pantograph passes under this component, it sets off a significant dynamic loading associated to high level of stress.

Figure 5a illustrates the contact wire fatigue fracture appearance obtained inline under a junction claw and Figure 5b shows that the contact wire rupture occurred at the boundary of the junction claw. However, the fatigue crack appearance is different from test bench: the origin of the crack failure took place under a junction claw on the lower edge of the contact wire. In other words, the crack initiation occurred on the sliding part.

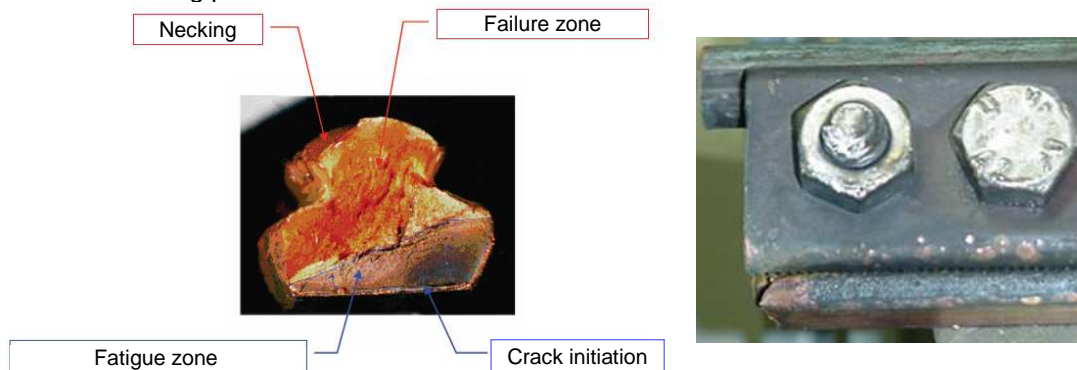


**Figure 5a. Inline CW fatigue fracture appearance under a junction claw; Figure 5b. Side view of a failure under a junction claw.**

In conclusion, the phenomena involved in the fatigue failure of the contact wire are very sensitive to environmental conditions. For instance under a junction claw, the stress fields are different:

- First, the clamping force applied by the junction claw to the wire exceeds 2kN/cm that has the effect of locally, but significantly, increasing the mean stress.
- Second, the dynamic stresses due to pantograph passage are strongly increased with the inertial effects added by the junction claw which generate a discontinuity of the apparent mass, The coupling of these phenomena makes the analysis of catenary fatigue complex.

Since it is impossible to perform tests on a bench with a junction claw, we attempted to simulate this phenomenon using a numerical model. Given the importance of having realistic stresses and the high difficulty of simulating the dynamic interaction between pantograph and catenary, OSCAR<sup>®</sup> is used because it is already validated and certificated.

### 3 OSCAR<sup>®</sup>: pantograph-catenary dynamic simulation

In the present section, we will first explain the complexity of the overhead line physics (also see [6], [7]), and then, how they are handled in the OSCAR<sup>®</sup> simulation software.

Firstly, the dynamic behaviour of the two flexible structures (the pantograph and the catenary) in sliding contact is very different in spite of having comparable stiffness. On one hand, the overhead line is a very long structure of wires, strongly prestressed in which bending waves propagate and, on the other hand, the pantograph is an articulated frame excited on two sides, by the train and by the overhead line, subjected to a disturbed aerodynamic environment.

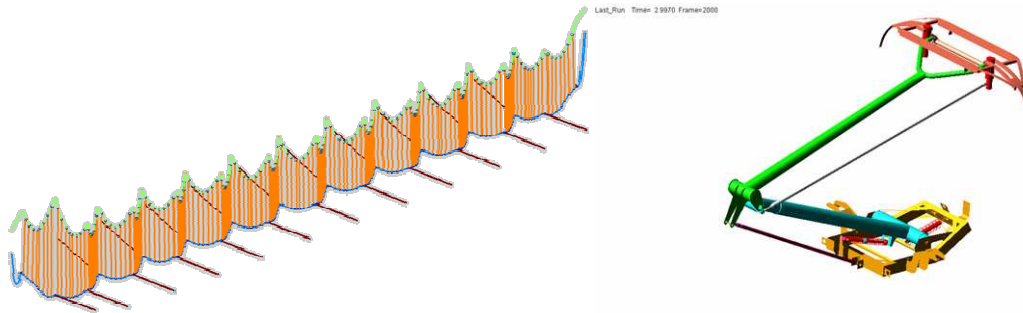


**Figure 6a. (left) Finite Element Catenary; Figure 6b. (right) Multibody pantograph.**

The sliding contact between these two flexible structures is the main difficulty in the modelling of the pantograph catenary dynamics. In OSCAR<sup>®</sup>, the overhead line is modelled using the Finite Element method and the contact with the pantograph is managed using the penalty method.

Secondly, pantograph-overhead line dynamics is particularly sensitive to the catenary static state. The computed static state is used to initialise the dynamic calculation and has consequently a very large impact on results. A realistic static state is however very complex to compute since it is highly non-linear. Indeed, the mechanical tension on the overhead line components involves high levels of stress and geometrical deflexions. In OSCAR<sup>®</sup>, the final geometry is obtained through a strongly non linear procedure which consists of solving iteratively

$$K(q_i) \cdot q_i = F_i,$$

where  $i$  is the iteration number,  $q$  is the displacement vector,  $K$  the stiffness matrix and  $F$  the force vector.

This procedure uses a progressive loading considering both the mechanical tension and the gravity. At each iteration  $i$ , the stiffness matrix is updated to consider the stress evolution in the whole overhead line and the convergence of displacements is finally ensured.

Prestressed beam formulations are used in order to take into account the additional stiffness due to mechanical tension. The equation below shows that the tension  $T$  has a big impact on the stiffness elementary matrix:

$$[K] = \sum_j \omega_j \left( \frac{1}{L} ES \frac{\partial N_u}{\partial r} \frac{\partial N_u}{\partial r} + \frac{1}{L} T \frac{\partial N_w}{\partial r} \frac{\partial N_w}{\partial r} + \frac{1}{L^3} EI \frac{\partial^2 N_w}{\partial r^2} \frac{\partial^2 N_w}{\partial r^2} \right)$$

This step plays a major role in the calculation of the mean stress in the contact wire. A validated computation is mandatory to obtain good results.

Other non-linearities appear in the system dynamics. First of all, the pantograph-catenary contact is unilateral, which can generate electrical arcs. The second non-linearity of the catenary is due to the droppers' unilaterality, as illustrated in the figure below, where one can notice that droppers do slacken at the pantograph passage.

Lastly, the overhead line is a wire structure of very big dimensions, strongly prestressed and very slightly damped. Bending waves propagate in the whole structure, reflect on different elements of the overhead line, and remain some minutes after the pantograph passage.

Damping modelling quality thus plays an important role in the software accuracy. OSCAR<sup>®</sup> uses a damping model based on Rayleigh hypothesis with different coefficients for each part of the overhead line (contact wire, messenger wire, droppers, steady arm, stitch wire):

$$C = \sum_i \alpha_i M_i + \beta_i K_i$$

where  $i$  is the index of the overhead line component group.

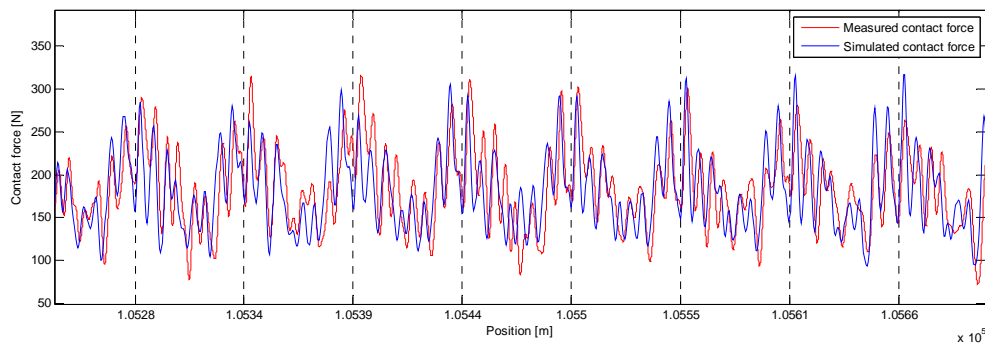


**Figure 7. Contact force correlation between simulation and measurements.**

Figure 7 presents the comparison between simulated contact force of OSCAR<sup>®</sup> (blue) and measurements (red). The good correlation of the both signals of contact force between the pantograph and the catenary confirms that loadings computed in OSCAR<sup>®</sup> can be used to study fatigue phenomena.

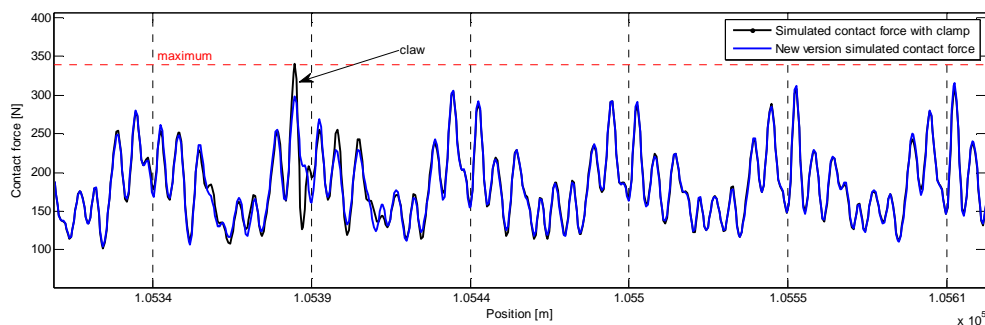


**Figure 8. Illustration of the contact force fluctuations due to junction claw using simulation tools.**

The Figure 8 illustrates the strong effect of junction claws on pantograph catenary dynamics. Indeed, the two curves are calculated with exactly same models. Only a junction was added in the black curve. Big fluctuations due to claw can be observed with the maximum value and maximum amplitude of the contact force. This modifications begins before the passage of the pantograph under the claw, this shows that it is mandatory to calculate stress cycle directly in OSCAR<sup>®</sup> because loading cycles are strongly related to operational conditions.

#### 4 Fatigue analysis

This section presents the whole procedure built to perform a fatigue analysis.

The loading path is a very sensitive parameter in fatigue study. For instance, the bending waves in catenary may influence the fatigue phenomenon. Therefore, a new functionality to study stresses in the contact wire was included in OSCAR<sup>®</sup> because it provides very predictive loading path.

It is necessary to study the multiaxial stresses because friction between the pantograph and the contact wire generates stresses upon plans xz and yz, the clamping force imposed by the junction claw may exceed 2kN/cm (the average stress in the contact wire is then heavily modified near this component) and last the junction claw applies a torsional stress caused by the swaying of the claw around the contact wire axis as drawn in the Figure 9.

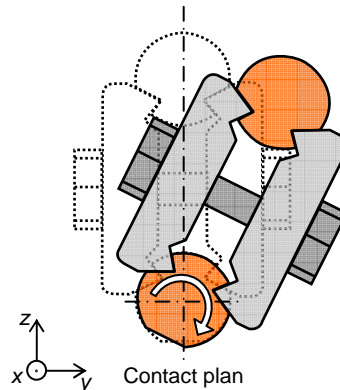


**Figure 9. Swaying of the claw around the contact wire axis.**

Therefore, it is necessary to work with a volume mesh of the contact wire to take into account all these phenomena. However, a volume mesh of the complete contact wire is impossible because the mesh refinement required here is very high.

OSCAR<sup>®</sup> uses one-dimensional (1D) finite elements. Thus, as a first step, longitudinal stress is studied using the 1D model to identify where the greatest stress is obtained along the OCL contact wire, for instance, near a support – where the stiffness is the most important – or rather at mid-span – where movements are important. This critical area in the catenary is studied using a volume mesh of the contact wire, like a zoom (see Figure 10), in order to limit required resources.

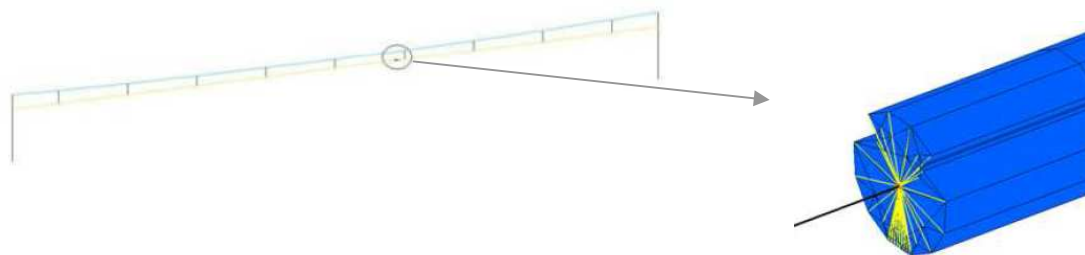


**Figure 10. Zoom on contact wire using a volume mesh.**

The dynamic interaction between pantograph and catenary is computed using only the 1D mesh that is fully validated. The volume mesh is used to obtain a fully three-dimensional representation of stresses corresponding to a multiaxial loading. The kinematics fields and strain fields from 1D calculation are imposed at boundaries and the contact force history is applied to the volume mesh to calculate multiaxial stresses.

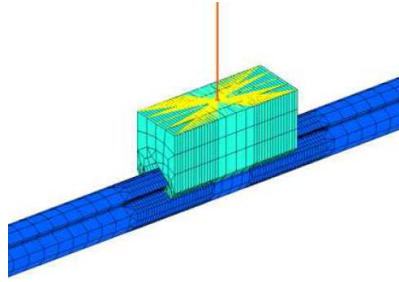


**Figure 11. Dropper claw and boundary conditions.**

For instance, the dropper claw requires an additional element corresponding to the dropper to take into account all boundary conditions as shown in the Figure 11.

The contact wire wear increasing with the number of cycle (corresponding to pantograph passage), fatigue and wear are strongly coupled [3]. Therefore, it is necessary to update the model because the mean stress, which is a critical parameter, changes with the wire section. First, the dynamic study made in OSCAR<sup>®</sup> takes into account the beam element properties changes due to mass and stiffness reduction. Second, the volume mesh is changed to obtain a realistic stress values.

#### 4.1 One dimensional analysis

The RTRI carried out inline tests to measure the bending strain amplitudes [2]. The strain waveform, given in Figure 12, is composed of a steep peak due to pantograph passage, preceded and followed by smaller amplitudes waves. Sugahara and all estimated the effect of accompanying waves on the fatigue life by using a waveform counting method described in [3].

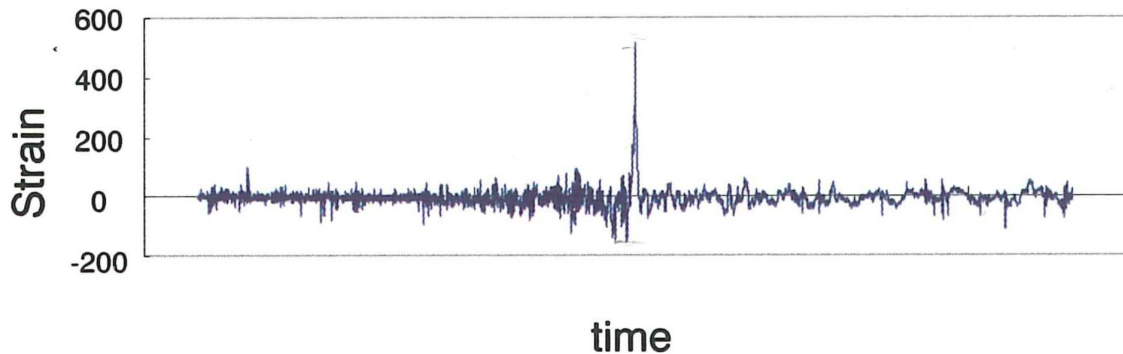


**Figure 12. Contact wire bending stress amplitude measured inline in Japan [3].**

The measured average is null because sensors were stuck on the upper surface of the inline contact wire. Thus the mean tensile strain exerted by the tensile load is not measured.

A simulation using OSCAR<sup>®</sup> was done to compare numerical results to this measurement. To reproduce this test conditions in OSCAR<sup>®</sup>, the stress  $\sigma_{xx}$  was calculated and the strain  $\varepsilon_a$  was deduced as

$$\varepsilon_a = \frac{\sigma_{xx} - \sigma_0}{E} \text{ where } \sigma_0 \text{ is the mean stress due to tension and } E \text{ is the hard copper Young modulus.}$$

OSCAR<sup>®</sup> being a finite element model using pretensionned Euler-Bernoulli beams and using generalized constraints, the longitudinal stress  $\sigma_{xx}$  is given by

$$\sigma_{xx}(x, y, z, t) = \frac{N}{S} - y \frac{M_z}{I_z} + z \frac{M_y}{I_y} = E(\varepsilon - y\kappa_z + z\kappa_y),$$

at any time  $t$  and for each point of the contact wire section using the coordinates  $(y, z)$ . In this way, as sensors were stuck on the upper surface of the contact wire, the study was performed for the point C represented in Figure 13.

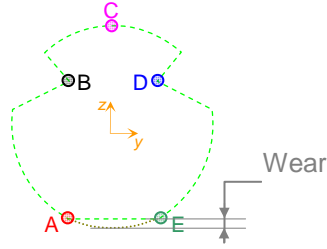


**Figure 13. Virtual contact wire section.**

The numerical result, illustrated in Figure 14, is different from measurements for waves which precede and follow the pantograph passage.

It can be explained by differences of French and Japanese catenaries and pantographs or by different damping ratio in catenary or by differences of frequency bandpass between measurements and software [8].

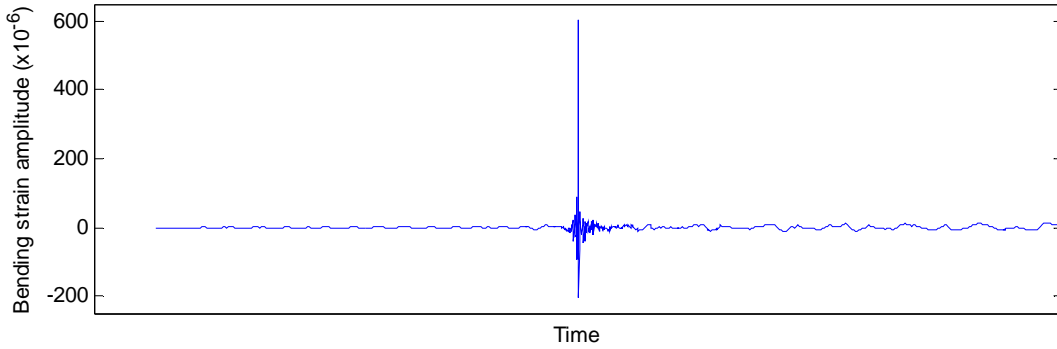


**Figure 14. Contact wire bending stress amplitude computed with OSCAR®.**

Nevertheless, the maximum and minimum bending strain amplitudes due to peak are similar and thus these results are good enough to make a preliminary fatigue analysis.

A criterion based on the Goodman's theory [9] is used, assuming an uniaxial loading. Although this assumption is not verified, it is applied in order to identify the most critical zone in the catenary as a preliminary study.

To apply this criterion, the maximum value and the minimum value of the longitudinal stress is calculated for each node of the mesh, using respectively

$$\Sigma_{\max} = \max_t \sigma_{xx}(x, y, z, t) \text{ and } \Sigma_{\min} = \min_t \sigma_{xx}(x, y, z, t).$$

Secondly, the criterion is applied and the point  $P(x, y, z)$ , corresponding to the maximum value of

$$\frac{\sigma_a}{2} + 0.3 \frac{\Sigma_{\max}}{3} \text{ is identified, with } \sigma_a(x, y, z) = \frac{\Sigma_{\max} - \Sigma_{\min}}{2}.$$

The criterion can be expressed in a better known form as:

$$\sigma_a + a\sigma_m < b$$

where  $a$  is the tensile strength and  $b$  is the fatigue limit.

The result of this study, applied on French catenary and shown in Figure 15, illustrates that the highest values of the criterion are closed to support represented by vertical dotted lines on Figure 15.

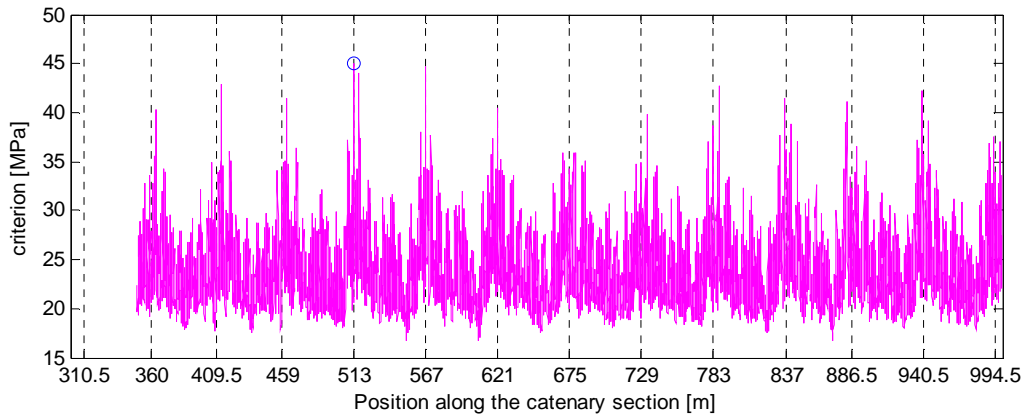


**Figure 15. Fatigue analysis using 1D criterion based on Goodman theory.**

As a conclusion, the main sensitive part of the catenary, regarding fatigue and using a 1D criterion, is close to supports.

#### 4.2 Three dimensional analysis

In this section, the 3D fatigue study is described. As it is explained before, the pantograph passage corresponds to one loading cycle and the related stress cycle is multiaxial because of the clamping force of claw junction and friction at the contact point. Therefore, the multiaxial Dang Van's criterion [10], which is a generalization of the Goodman's criterion to a multiaxial stress cycle, is used. It is written as

If  $\max_t \{ \tau(t) + a \cdot p(t) \} < b$  there will not take place a crack initiation.

- $p(t) = \frac{1}{3}(\sigma_{11}(t) + \sigma_{22}(t) + \sigma_{33}(t))$  is the hydrostatic pressure
- $\tau$  is the shear stress amplitude at mesoscopic scale
- $a$  and  $b$  are two material parameters determined from the endurance limits

This criterion is generally represented in the  $(\tau(t), p(t))$  diagram given in Figure 16.

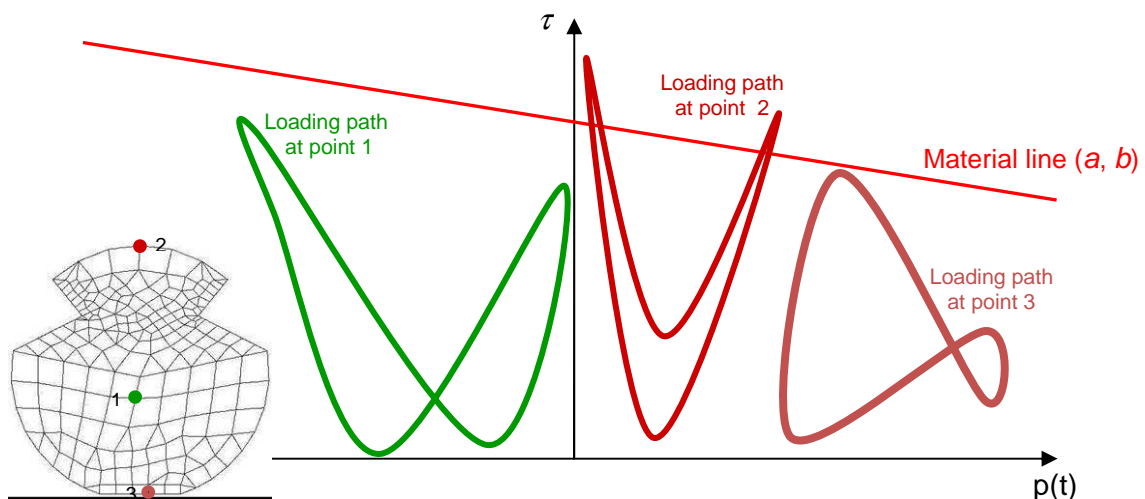


**Figure 16. Dang Van Diagram theory description.**

It is applied at each node of the volume mesh in order to identify which are critical for fatigue. All loading paths are plotted in the diagram and if one loading path exceeds the threshold given by the material line  $(a, b)$ , a crack initiation may occur. Otherwise, with none loading path over the material line, the component has a unlimited lifetime.

To apply the Dang Van's criterion to catenary, it was necessary to build volume meshes for each configuration including different types of claws. In order to limit the size of claw meshes, their geometry was simplified and a mechanically equivalent component is meshed, as shown in Figure 17.

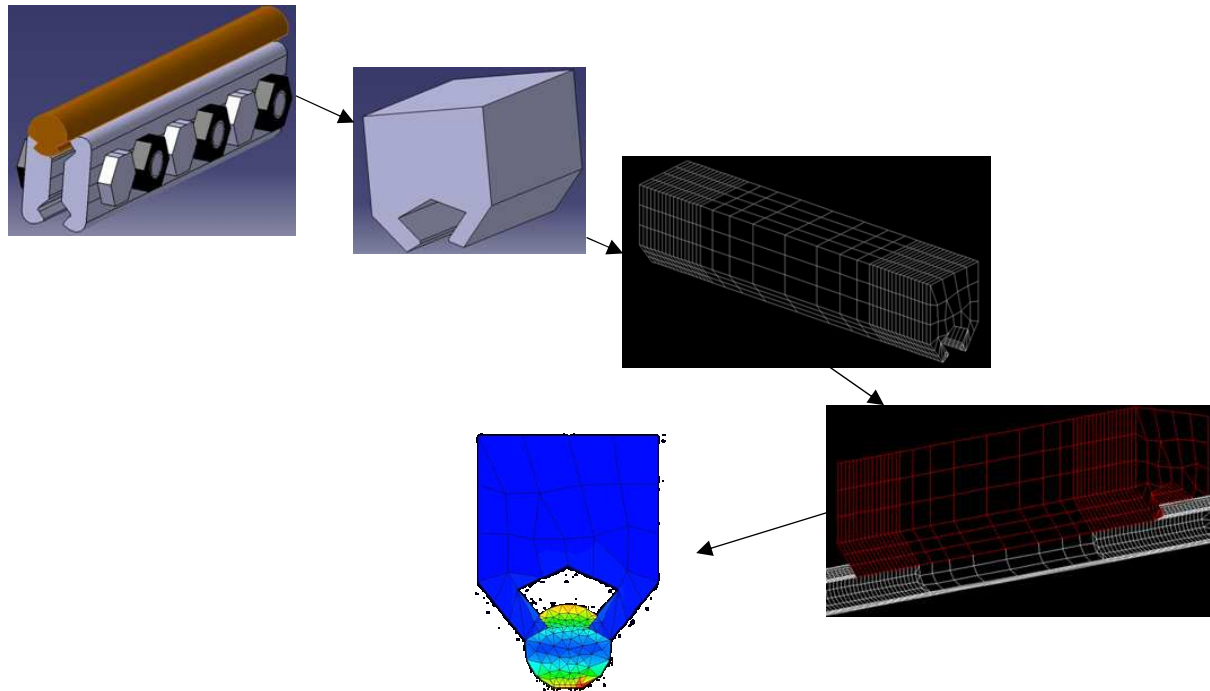


**Figure 17. Procedure to build volume mesh with a junction claw.**

The image at the bottom in Figure 17 represents isovalues of stress obtained in the contact wire, using FE analysis. The junction claw is considered as a non-deforming component. The stress tensor obtained can be used to perform a fatigue analysis by making a cumulative damage.

## 5 Conclusion

The proposed article deals with fatigue in the Overhead Contact Line (OCL) applied to a typical French catenary. This system failure is critical for railways operators. An analysis of the different parameters that significantly influence the fatigue phenomenon is carried out in this study.

First, a preliminary analysis based on experimental results shows that involved phenomena are complex, particularly because of coupling of dynamics and wear, and because they are very sensitive to condition of use.

Then, to ease understanding of these phenomena, a numerical study was made. The followed procedure is presented here. In order to use the very accurate results of dynamic interaction given by software OSCAR<sup>®</sup>, new functionalities were developed to determine stresses fields in the catenary. The fatigue study is divided into two steps, first a 1D study is carried out to localise the critical area in catenary and then a volume mesh of the contact wire is built to particularly study junction claws, a component used in catenary maintenance which has triggered some incidents in France. Indeed, it is shown in this paper that the loading path is multiaxial and thus three dimensional models are necessary.

Finally, an introduction to fatigue cycling based on the Dang Van's criterion is presented.

## 6 Acknowledgments

This paper describes work undertaken in the context of the partnership between SNCF and RTRI. These fruitful exchanges have allowed discussions on methods and different approaches. We particularly emphasize the useful tests conducted by the RTRI to characterize the SNCF contact wire. Moreover, the authors thank S. Daouk for the good work he did during his internship.

## 7 References

- [1] C. Yamashita, A. Sugahara, "Influence of Mean Stress on Contact Wire Fatigue", QR of RTRI, Vol. 47, No. 1, Feb. 2006.
- [2] A. Sugahara, "Preventing Fatigue Breakage of Contact Wires", Railway Technology Avalanche No. 24, September 19, 2008.
- [3] A. Sugahara, C. Yamashita, T. Usuki, "Applicability of Rain Flow Method to Fatigue Life Span Estimation of Overhead Contact Wire", QR of RTRI, Vol. 51, No. 4, Nov. 2010.
- [4] L.M. Cléon, A. Bobillot, J.P. Mentel, E. Aziz: "OSCAR<sup>®</sup>: La caténaire en 3D". In: Revue Générale des Chemins de Fer, Volume n°155, Novembre r 2006.
- [5] S. Daouk, "Analyse en fatigue du fil de contact de la caténaire", master report ENSTA/SNCF, 2010
- [6] A. Bobillot, L.M. Cléon, A. Collina, O. Mohamed, R. Ghidorzi, "Pantograph-Catenary: a High-Speed European couple". In: Proceedings of the World Congress on Railway Research, 2008.
- [7] J.P. Massat, "Modélisation du comportement dynamique du couple pantographe-caténaire. Application à la détection de défauts dans la caténaire", doctoral thesis 2007.
- [8] J.P. Bianchi, E. Balmès, A. Bobillot, "Using modal damping for full model transient analysis. Application to pantograph/catenary vibration", ISMA2010 Noise and Vibration Engineering conference 2010.
- [9] K. Dang Van and H. Maitournam, "Fatigue Polycyclique des Structures", support de cours école polytechnique, Décembre 2008.
- [10] K. Dang Van and I. Papadopoulos, Eds., "High-Cycle Metal Fatigue in the Context of Mechanical Design", CISM Courses and Lectures, No.392, Springer-Verglas, 1999.